Analyst

Interdisciplinary detection science

www.rsc.org/analyst

Volume 134 | Number 3 | March 2009 | Pages 409–620

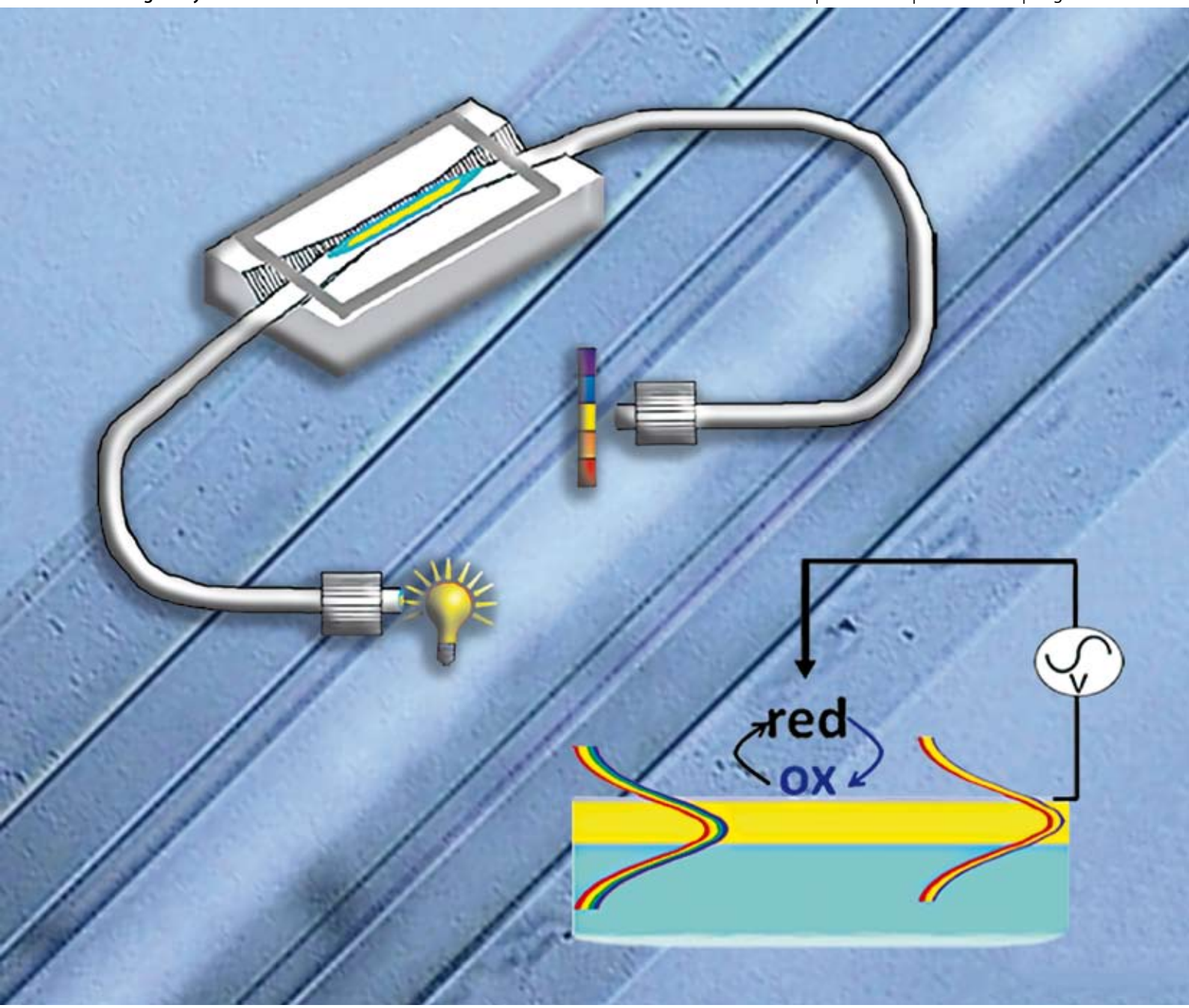

ISSN 0003-2654

RSC Publishing

0003-2654(2009)134:3;1-H

An electroactive fiber optic chip for spectroelectrochemical characterization of ultra-thin redox-active films

Brooke M. Beam,[b] Neal R. Armstrong[b] and Sergio B. Mendes*[a]

Received 21st August 2008, Accepted 21st November 2008
First published as an Advance Article on the web 19th December 2008
DOI: 10.1039/b814338b

The first, fully integrated, planar fiber optic platform with spectroelectrochemical capabilities, termed the electroactive fiber optic chip (EA-FOC) is presented here. Spectroelectrochemical techniques provide complementary optical and electrochemical data which are important for applications ranging from thin film characterization to advanced sensor design. To create the EA-FOC a side-polished fiber optic is coated with a thin film of indium-tin oxide (ITO) as the working electrode and used to probe electrochemically-driven changes in absorbance for surface-confined redox species. A sensitivity enhancement of ~40 times higher than a transmission measurement is demonstrated for this first-generation EA-FOC, using the methylene blue (MB) redox couple, cycling between the visibly colored, oxidized form of MB, and its leuco (transparent) reduced form. Additionally, the EA-FOC is used to probe the redox spectroelectrochemistry of an electrodeposited thin film, about 0.3% of a monolayer, of the conducting polymer poly(3,4-ethylenedioxythiophene) (PEDOT). Unlike other waveguide formats, the EA-FOC offers an ease of use due to its ability to simply couple to light sources and detectors through standard fiber connectors to create a sensitive planar waveguide spectroelectrochemical platform.

Introduction

Spectroelectrochemical techniques are routinely used to characterize redox mechanisms of solution probe molecules,[1,2] redox processes of ultra-thin films of conducting polymers,[3,4] and electrochemical processes in adsorbed protein films.[5,6] Measuring optical changes that are coincident with the redox event provides several significant advantages, mainly arising from the fact that these optical changes occur independently of non-Faradaic processes at the electrode/solution interface. Monitoring changes in absorbance or reflectance as a function of applied potential provides optical data that can be used to reconstruct the current flowing solely in the Faradaic event without the capacitive current background, which can often be larger than the Faradaic current especially for ultra-thin redox films. When the optical characterization is carried out on a waveguide platform, overcoated with a transparent electrode material (*e.g.* indium-tin oxide, tin oxide, boron-doped diamond, *etc.*),[7–12] there can be significant sensitivity enhancement relative to transmission spectroelectrochemical experiments due to the increased optical pathlength of the platform. This sensitivity enhancement is often sufficient to allow for characterization of electron transfer events at sub-monolayer coverages of the redox-active molecular system and may provide information about structural changes which occur during electron transfer.[4,6,13,14] Additionally, multifunctional spectroelectrochemical platforms are used for advanced sensor technologies requiring the greater flexibility of the combined electrochemical and spectroscopic techniques in sensor architecture design.[15,16]

Over the last decade the sensitivity of spectroelectrochemical measurements have been significantly enhanced by using monochromatic and broadband attenuated total reflectance (ATR),[8,17–19] multi-mode waveguides,[11,20–22] and single-mode waveguides.[7,10] These technologies follow on the original work of Winograd and Kuwana using monochromatic ATR platforms which demonstrated a ~7-fold increase in sensitivity compared to transmission spectroelectrochemical measurements.[18] Itoh and Fujishima subsequently demonstrated that a tin oxide film coating on a 2 μm thick single-mode, gradient index channel waveguide increased the sensitivity of spectroelectrochemical measurements of a surface-confined molecule (methylene blue – MB) by ~150 times.[11] A significant advance has been the introduction of the electroactive integrated optical waveguide (EA-IOW) platform,[9,10] which is a single-mode, step-index guide, overcoated with 25–50 nm of indium-tin oxide (ITO), and shows the highest spectroelectrochemical sensitivity (relative to a transmission experiment) yet reported of $10^3\times$ and up to $10^4\times$.

A significant hindrance for these ATR and EA-IOW spectroelectrochemical technologies, however, has been interfacing the internal reflection element (IRE) with standard, commercially available spectroscopic instrumentation. Optical coupling in and out of a planar waveguide platform requires precision optics, tight mechanical tolerances, time-consuming alignment, and for some configurations, advanced micro-optics fabrication technologies, such as integrated diffraction gratings.[7,23] Only one field-portable instrument has been developed, by Heinemann and co-workers, based on an ATR configuration and used to spectroelectrochemically detect ferrocyanide.[24,25]

Fiber optic-based spectroscopic devices, however, have the advantage of being extremely easy to couple light into and out-of,

[a]*Department of Physics and Astronomy, University of Louisville, Louisville, Kentucky 40292, USA. E-mail: sbmend01@louisville.edu; Fax: +1-502-852-8128*
[b]*Department of Chemistry, University of Arizona, Tucson, Arizona 85721, USA*

using fiber-coupled sources; thus, leading to the growing number of applications for fiber optic-based devices as chemical sensors.[26,27] UV-Vis,[28] FTIR,[29] and Raman[30] fiber-coupled spectroelectrochemical measurements have been obtained using the distal end of a fiber optic probe as the working electrode. These fiber optic probes suffer from some of the same shortcomings of transmission absorbance spectroelectrochemical measurements – they are limited by the short optical path length of the measurement. Combining the increased sensitivity and surface specificity of an electroactive waveguide with the simplicity of a fiber-coupled spectroscopic device, into a fully integrated fiber optic-based spectroelectrochemical platform, would potentially have a broad range of spectroelectrochemical sensing applications.

Toward this end, we recently introduced a multi-mode side-polished fiber platform, called the Fiber Optic Chip (FOC), for broadband absorbance and fluorescence measurements.[31] The FOC features a region where about half of the fiber core and cladding has been removed by a side-polishing procedure to form a planar sensing region. The FOC combines the advantages of a planar waveguide platform, and the ease of in- and out-coupling of fiber-coupled broadband light sources and multi-channel detectors. The current generation of FOC platforms has a sensitivity enhancement of 25–50 times compared to transmission experiments, analogous to ATR measurements, but with a much simpler interface with spectroscopic equipment.

In this article we present the first fully integrated fiber-coupled spectroelectrochemical IRE platform, termed the electroactive fiber optic chip (EA-FOC). To create the EA-FOC we coat the FOC with a thin film of indium-tin oxide (ITO) as the working electrode (Fig. 1), and use this technology to probe electrochemically-driven changes in absorbance for surface-confined redox species. A sensitivity enhancement of ~40 times a transmission measurement is demonstrated for this first-generation EA-FOC, using the methylene blue (MB) redox couple, cycling between the visibly colored, oxidized form of MB, and its leuco (transparent) reduced form. We also demonstrate the properties of the EA-FOC by probing the redox spectroelectrochemistry of an electrodeposited film of the conducting polymer poly(3,4-ethylenedioxythiophene) (PEDOT). The EA-FOC, when fully optimized, will offer an ease of use not available in other waveguide formats, especially the simplicity with which the entire visible wavelength region can be interrogated during redox events of surface-confined molecular species.

Experimental

The electroactive fiber optic chip (Fig. 1) consists of a side-polished multi-mode optical fiber mounted in a glass V-groove support. The fabrication process, including the polishing steps required to create a planar waveguide surface, with minimized light scattering and related optical losses, are described in detail in earlier papers.[31,32] For the experiments reported here, a 50 μm core diameter, step-index, multi-mode fiber (Thorlabs AFS50/125Y), with a 125 μm cladding diameter and a numerical aperture (NA) of 0.22, was mounted into a glass V-groove (Mindrum) using thermally curing epoxy (Epotek 301), and polished to expose the fiber core, providing an interaction length for the spectroelectrochemical experiments of 19.4 ± 0.8 mm and a width of 50 μm. Once polished the FOC platform is

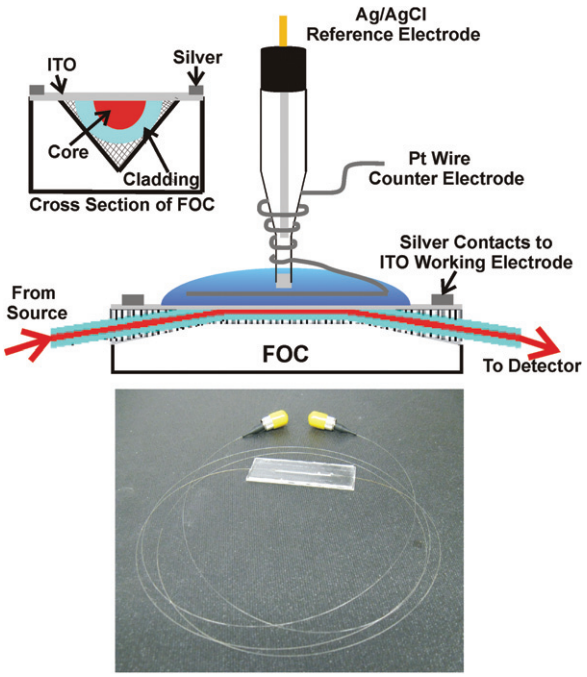

Fig. 1 Schematic of the experimental set-up for the EA-FOC and a picture of an EA-FOC. Silver epoxy is used to make electrochemical contact with the ITO film working electrode. A Ag/AgCl reference electrode is wrapped with Pt wire to create a counter electrode and brought into contact with the electrolyte solution to complete the electrochemical cell. Inset shows a cross-section view of the EA-FOC.

characterized by measuring the absorbance of a self-assembled polyelectrolyte film,[31] to verify its sensitivity as a waveguide platform.

The FOC was next coated with an ITO layer of *ca.* 40 nm thickness. The philosophy behind the addition of the ITO layer is much the same as in previous work reported[7,9,10] – the ITO layer needs to be of sufficient thickness to provide the electroactivity needed for good electrochemical response, but must remain thin and defect-free so as to keep the optical throughput of the FOC optimized. The ITO film was sputtered onto the surface of the FOC using a Kurt J. Lesker AXXIS pulsed DC magnetron sputter deposition system. The base vacuum pressure was 2×10^{-6} Torr, and an atmosphere of Ar with 3.3% O_2 was maintained with a pressure of 8.5 mTorr during ITO sputter deposition. The In_2O_3/SnO_2, 90/10% wt, 3 inch diameter target was sputtered at 200 W for 4 minutes to produce a 40 nm thick film of ITO. After deposition, the EA-FOC was annealed in 10 minute increments at 300 °C under vacuum, to produce an effective sheet resistance of 2000 Ω/□. ITO film thickness was verified using AFM (Digital Instruments Dimension 3100, tapping mode) to measure the step height of a partially acid etched film deposited onto another FOC platform under the same conditions. A portion of the ITO was masked using ParaFilm© to protect against etching, and the remainder of the ITO was acid etched in a 6 M HCl (EMD) 0.2 M $FeCl_3$ (EM Science) aqueous solution for 5 minutes.[33] The extinction coefficient was estimated to be 5×10^{-3} at 500 nm (which is equivalent to an estimated propagation loss of ~0.5 dB/cm) using interference fringes of a thick ITO film deposited under the same conditions.[34,35]

A home-built fiber-coupled light source was used in all experiments reported here. The light from a Xe-arc lamp (Oriel) was reduced with an iris and was focused onto a fiber using a lens (focal length = 50.2 mm; with 1 : 1 imaging magnification). Therefore, the EA-FOC could simply be plugged into the broadband source for spectroscopic measurements using standard fiber connectors. The other end of the EA-FOC was fiber-coupled into a spectrometer (SI Photonics 430) using a fiber collimating lens (Thorlabs, focal length = 11 mm) and a focusing lens (focal length = 50.2 mm) into a collection fiber (SI Photonics, 400 μm core); appropriate neutral density filters were placed between the two lenses and perpendicular to the beam of light. However, it is entirely feasible and straightforward to replace our laboratory optical set-up employed for the measurements presented here with commercially available fiber-coupled light sources and detectors using the EA-FOC platform.

Spectroelectrochemical measurements were made in a sample well surrounding the exposed fiber core. Electrical contact with the EA-FOC was made using silver epoxy (SPI) painted around the edge of the V-groove; two platinum wires (Sigma) were attached bordering both ends of the exposed core to provide contact of the working electrode to the potentiostat, minimizing iR drop across the ITO film. Kapton (3M) tape was used to mask the evanescent sensing region of the EA-FOC (19.5 × 1 mm) and the whole structure was backfilled with Sylgard 183 (Dow) poly(dimethylsiloxane) (PDMS). The PDMS gasket created the sample well, which isolated the electrolyte solution from the silver contacts on the surface of the FOC. The outside of the Ag/AgCl (BAS) reference electrode was wrapped with platinum wire to provide a counter electrode in close proximity to both reference and working electrodes, and brought into contact with the electrolyte solution on top of the EA-FOC to complete the electrochemical cell (Fig. 1). A potentiostat (CHI Instruments 660) collected electrochemical measurements and maintained potential control of the EA-FOC. The EA-FOC was cleaned before all measurements by scrubbing with a 10% Triton-X solution and a microfiber cloth, rinsing with Millipore water, rinsing with ethanol and drying with a stream of N_2.

Methylene blue (MB, Sigma) solutions in 0.1 M KNO_3 (Sigma) were prepared at concentrations of 15, 50, 80, and 100 μM. The EA-FOC was first cycled in electrolyte solution 10 times over the potential region of interest to suppress both electrochemical and optical hysteresis of the ITO film.[10] For spectroelectrochemical measurements, the MB solutions were incubated in the sample well for 10 minutes. The EA-FOC potential was scanned from 0.1 V to −0.4 V and back at a rate of 10 mV/s. Spectra were recorded every 40 mV and the absorbance was calculated using reference spectra taken for the electrolyte solution at the same potential. The sample well was then flushed with about 10 cell volumes of electrolyte solution before introduction of the next MB solution. Electrochemical polymerization of PEDOT onto the surface of the EA-FOC was carried out by stepping the potential of the EA-FOC to 1.1 V in 10 mM 3,4-ethylenedioxythiophene (EDOT, Aldrich) with 0.1 M $LiClO_4$ (Aldrich) 10% methanol aqueous solution.[36] We estimate the PEDOT film to be *ca.* 0.3% of a monolayer assuming $\varepsilon = 3.6$ cm^2/nmol[36] and an area of 10 Å^2 per EDOT unit.[37] Spectroelectrochemical measurements were collected by scanning the potential from 0.5 V to −0.8 V, and back, at 10 mV/s, recording spectra every 40 mV.

Results and discussion

The MB redox couple was chosen to evaluate the sensitivity of the EA-FOC to potential-driven absorbance changes. The spectroelectrochemistry of adsorbed monolayers of MB has been

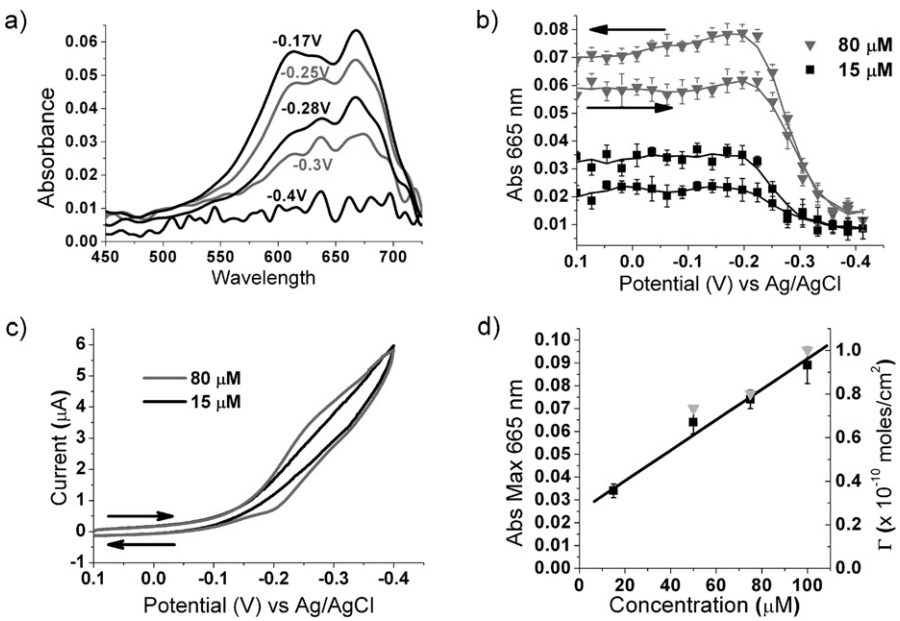

Fig. 2 (a) Broadband absorbance spectra at several potentials for an MB film adsorbed onto the EA-FOC from an 80 μM solution. (b) Absorbance of MB at 665 nm on the EA-FOC with respect to potential for 15 (■) and 80 (▼) μM solution concentrations. (c) CVs of MB films deposited from 15 (black line) and 80 μM (gray line) solutions. (d) Correlation of EA-FOC measured absorbance (■) with electrochemically determined surface coverage (▼) *versus* bulk solution MB concentration.

previously established on IOW[10,11] platforms; therefore, the MB redox couple is used for comparison of the EA-FOC with these well-known techniques. MB electrostatically adsorbs to the ITO surface in its native oxidized form at coverages from sub-monolayer up to monolayer, depending upon solution concentrations. Surface-adsorbed MB undergoes a chemically reversible 2-electron reduction to the transparent leuco form of the dye at *ca.* −0.27 V *versus* a Ag/AgCl reference electrode. For the micromolar solution concentrations used in this study, the bulk MB absorbance does not contribute appreciably to the EA-FOC spectroelectrochemical response.

Fig. 2a shows the broadband absorbance spectra recorded using the EA-FOC at several potentials, in a solution of 80 μM MB, where the absorbance maxima for both the monomer (665 nm) and aggregate forms of this dye (605 nm) are present.[38] Fig. 2b is a plot of the absorbance of the monomer at 665 nm *versus* potential as the potential is scanned from 0.1 V to −0.4 V and back to 0.1 V. The optical absorbance changes for 80 μM and 15 μM MB are easily detected. As the potential is scanned more negative (forward sweep), the absorbance decreases as the MB film is reduced to the transparent leuco form of the dye. Upon scan reversal the oxidized forms of MB reappear with some increase in absorbance intensity. This kind of hysteresis has been observed previously for the characterization of MB redox chemistry on the EA-IOW platform, at slow sweep rates only.[9,10] The hysteresis has been attributed to re-oxidation of a higher coverage of MB created as a result of the reduction of the initially adsorbed material, and diffusion-controlled adsorption of new MB in concert with the reduction of the initial adsorbed MB. If faster sweep rates are used, the absorbance changes for both forward and reverse sweeps are similar and no hysteresis or indication of increased MB coverage was seen.

For the complementary voltammograms collected for the same MB concentrations (Fig. 2c), the Faradaic voltammetric signal is small and difficult to resolve above the steeply sloping background for the 80 μM solution of MB, and impossible to see above background for an MB concentration of 15 μM or lower. The large background current due to non-Faradaic processes (*i.e.* double layer capacitance and redox processes which are not associated with the redox chemistry of MB) makes characterization of Faradaic processes difficult using only current detection; hence, the desire to use low background spectroelectrochemical measurements such as demonstrated here for the EA-FOC.[10]

After background subtraction, the voltammetric peak area for 50, 80, and 100 μM MB solutions was determined and used to calculate surface coverage of MB on the EA-FOC. For the 80 μM solution, the surface coverage was calculated to be 8.0×10^{-11} mole/cm^2, which corresponds to 30% of a full monolayer based on a molecular area of 66 Å^2/molecule.[39] Both the calculated surface coverage and the corresponding measured absorbance are directly proportional to the MB solution concentration, as can be seen in Fig. 2d. The sensitivity of the EA-FOC can then be calculated using the electrochemically determined surface coverage and the experimentally measured absorbance for these three solutions, using the Beer's law relationship $A = S\varepsilon\Gamma$, where S is the EA-FOC sensitivity factor, ε is the molar absorptivity, and Γ is the surface coverage of MB. The molar absorptivity is assumed to be the same as for MB in solution, 2.2×10^4 M^{-1} cm^{-1} at 665 nm.[39] The sensitivity of the EA-FOC was calculated to be 40 ± 2 or 20.6/cm, which is comparable to sensitivities seen for our first-generation FOC platform.[31]

Finally, the EA-FOC was used to electrochemically polymerize ultra-thin films of PEDOT, and probe the spectroelectrochemical characteristics of the polymer film as a further proof of its sensitivity to redox events for surface-confined species. We electropolymerized PEDOT over the entire coated ITO region, by means of potential step electrodeposition as described elsewhere.[36] The coverage of PEDOT in the evanescent field region was estimated to be *ca.* 0.3% of a monolayer, or 4.3×10^{-12} mole/cm^2, assuming $\varepsilon = 3.6$ cm^2/nmol[36] and an area of 10 Å^2 per EDOT unit.[37] PEDOT undergoes a reversible oxidation from the neutral dark blue form of the polymer to the almost transparent single polaron state, and upon further oxidation to the bipolaron form of the polymer.[40] The reduction/oxidation voltammogram of the electrodeposited PEDOT film on the EA-FOC shows broad voltammetric peaks, poorly distinguishable from the background current (Fig. 3a). The spectroelectrochemical measurement of the change in absorbance at the λ_{max} (550 nm) *versus* potential illustrates the electrochromic behavior of the PEDOT film (Fig. 3b). In Fig. 3c the first derivative of the absorbance change

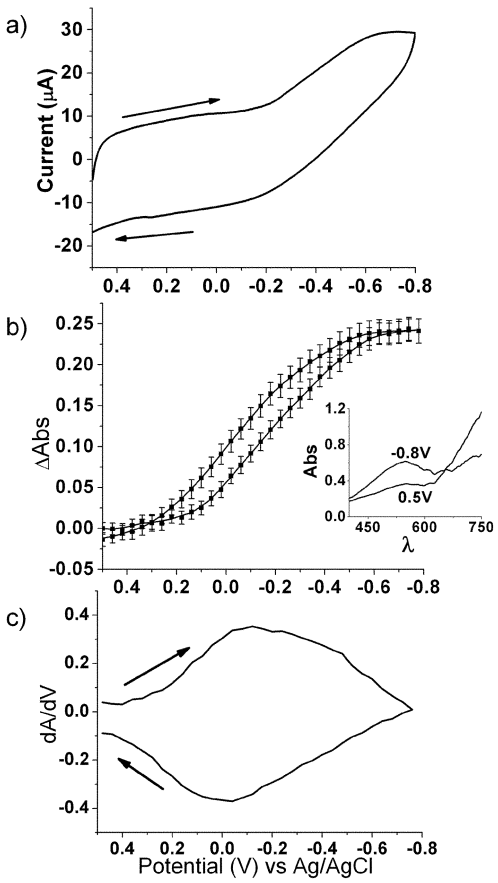

Fig. 3 (a) CV of PEDOT film on the EA-FOC at 10 mV/s; (b) absorbance difference (at 550 nm) *versus* potential for PEDOT film on the EA-FOC (inset: broadband absorbance spectra for reduced PEDOT at −0.8 V and oxidized polymer at 0.5 V *versus* Ag/AgCl on the EA-FOC); (c) absorptovoltammogram for the same ultra-thin PEDOT film, at 10 mV/s.

(at 550 nm) as a function of varying potential is plotted, to create the absorptovoltammetric response.[10,41] The cathodic transition is represented by the upper portion of this plot; the lower portion of this plot corresponds to the anodic wave. As expected from previous absorptovoltammetric experiments, the electrochemical events are much better resolved from background using optical characterization. The peak separation (ΔE_{peak}) and the standard redox potential (E°) is determined to be −0.12 V and −0.06 V *versus* Ag/AgCl respectively from the absorptovoltammogram, correlating well with the published electrochemical E° of ~0 V *versus* Ag/AgCl.[40] The results from this study do not indicate the oxidized form of the polymer, polaron or bipolaron, because the absorptovoltammogram is only monitoring the appearance/disappearance of the neutral polymer. The optical changes from the transition from polaron to the bipolaron are less pronounced and occur at longer wavelengths than the current experimental set-up allows.[40] Nevertheless, it is clear that the EA-FOC has the requisite sensitivity to monitor optical changes to such redox-active polymer films, down to surface coverages of *ca.* 0.3% of a monolayer.

Conclusions

We have demonstrated a new spectroelectrochemical platform which has many of the desirable features of planar waveguides, and the convenience of fiber optic coupling for the broadband spectroscopic characterization of ultra-thin films of redox-active materials. As with the first-generation FOC counterpart, this version of the EA-FOC shows a sensitivity improvement over transmission experiments of *ca.* 40×. The sensitivity of the device, analogous to the FOC platform, can be doubled by simply inserting an annular mask in the optical pathway.[31] We anticipate further improvements in sensitivity will be possible by increasing the interaction length of the device and generating an EA-FOC based on a single-mode side-polished fiber. Planar waveguide formats are more desirable than using the distal end of an optical fiber for characterization of planar supported thin films (*e.g.* biofilms, lipid bilayers, *etc.*).[3,13,16,42] The major appeal of the EA-FOC, however, lies in the combination of these planar waveguide characteristics with the ease of fiber optic in- and out-coupling of light over a broad spectral region, and the compatibility with multi-channel spectroscopic detection capabilities. UV-grade fibers have also recently been explored for FOC platforms,[43] and there is no fundamental reason that the EA-FOC could not be extended to near- and even mid-IR spectroelectrochemical platforms, using conducting overlayers which have sufficient transmittance in these spectral regions.[29] Work in progress seeks to expand the sensor capabilities of these new platforms, and increase both their sensitivity and their ease of use over broad spectral ranges.

Acknowledgements

The authors would like to thank Jill Craven for her help with FOC fabrication. This work was supported by the National Science Foundation under Grants Number DBI-0352449 (SBM) and CHE-0517963 (NRA) and the Science and Technology Center-Materials and Devices for Information Technology Research Grant Number DMR-0120967 (NRA). BMB acknowledges fellowship support from a TIRF Proposition 301 (Arizona) Graduate Fellowship in Photonics.

References

1 T. Kuwana and N. Winograd, in *Electroanalytical Chemistry*, ed. A. Bard, Marcel Dekker, Inc., New York, 1974, vol. 7, pp. 1–78.
2 W. R. Heineman, F. M. Hawkridge and H. N. Blount, in *Electroanalytical Chemistry*, ed. A. Bard, Marcel Dekker, Inc., New York, 1984, vol. 13, pp. 1–113.
3 C. Ge, N. R. Armstrong and S. S. Saavedra, *Anal. Chem.*, 2007, **79**, 1401–1410.
4 C. Ge, W. J. Doherty III, S. B. Mendes, N. R. Armstrong and S. S. Saavedra, *Talanta*, 2005, **65**, 1126–1131.
5 F. M. Hawkridge and I. Taniguchi, *Comments Inorg. Chem.*, 1995, **17**, 163–187.
6 Z. O. Araci, A. F. Runge, W. J. Doherty and S. S. Saavedra, *J. Am. Chem. Soc.*, 2008, **130**, 1572–1573.
7 J. T. Bradshaw, S. B. Mendes, N. R. Armstrong and S. S. Saavedra, *Anal. Chem.*, 2003, **75**, 1080–1088.
8 W. J. Doherty, C. L. Donley, N. R. Armstrong and S. S. Saavedra, *Appl. Spectrosc.*, 2002, **56**, 920.
9 D. R. Dunphy, S. B. Mendes, S. S. Saavedra and N. R. Armstrong, in *Interfacial Electrochemistry: Theory, Experiment and Applications*, ed. A. Wieckowski, Marcel Dekker, Inc., New York, 1999, pp. 513–525.
10 D. R. Dunphy, S. B. Mendes, S. S. Saavedra and N. R. Armstrong, *Anal. Chem.*, 1997, **69**, 3086–3094.
11 K. Itoh and A. Fujishima, *J. Phys. Chem.*, 1988, **92**, 7043–7045.
12 J. Stotter, J. Zak, Z. Behier, Y. Show and G. M. Swain, *Anal. Chem.*, 2002, **74**, 5924–5930.
13 A. F. Runge, S. B. Mendes and S. S. Saavedra, *J. Phys. Chem. B*, 2006, **110**, 6732–6739.
14 A. F. Runge, N. C. Rasmussen, S. S. Saavedra and S. B. Mendes, *J. Phys. Chem. B*, 2005, **109**, 424–431.
15 A. B. Ellis and D. R. Walt, *Chem. Rev.*, 2000, **100**, 2477–2478.
16 T. W. McBee, L.-Y. Wang, C. Ge, B. M. Beam, A. L. Moore, D. Gust, T. A. Moore, N. R. Armstrong and S. S. Saavedra, *J. Am. Chem. Soc.*, 2006, **128**, 2184–2185.
17 W. N. Hansen, T. Kuwana and R. A. Osteryoung, *Anal. Chem.*, 1966, **38**, 1810–1821.
18 N. Winograd and T. Kuwana, *J. Electroanal. Chem.*, 1969, **23**, 333–342.
19 N. Winograd and T. Kuwana, *J. Am. Chem. Soc.*, 1971, **93**, 4343–4350.
20 K. Itoh and A. Fujishima, in *Electrochemistry in Transition*, ed. O. J. Murphy, S. Srinivasan and B. E. Conway, Plenum Press, New York, 1992, pp. 219–225.
21 S. E. Ross, C. J. Seliskar and W. R. Heineman, *Anal. Chem.*, 2000, **72**, 5549–5555.
22 C. Piraud, E. Mwarania, G. Wylangowski, J. Wilkinson, K. O'Dwyer and D. J. Schiffrin, *Anal. Chem.*, 1992, **64**, 651–655.
23 S. B. Mendes, L. Li, J. J. Burke, J. E. Lee, D. R. Dunphy and S. S. Saavedra, *Langmuir*, 1996, **12**, 3374–3376.
24 M. L. Stegemiller, W. R. Heineman, C. J. Seliskar, T. H. Ridgway, S. A. Bryan, T. Hubler and R. L. Sell, *Environ. Sci. Technol.*, 2003, **37**, 123–130.
25 D. J. Monk, T. H. Ridgway, W. R. Heineman and C. J. Seliskar, *Electroanalysis*, 2002, **15**, 1198–1203.
26 A. Leung, P. M. Shankar and R. Mutharasan, *Sens. Actuators, B*, 2007, **125**, 688–703.
27 C. McDonagh, C. S. Burke and B. D. MacCraith, *Chem. Rev.*, 2008, **108**, 400–422.
28 D. A. VanDyke and H.-Y. Cheng, *Anal. Chem.*, 1988, **60**, 1256–1260.
29 M. J. Shaw and W. E. Geiger, *Organometallics*, 1996, **15**, 13–15.
30 S. D. Schwab, R. L. McCreery and F. T. Gamble, *Anal. Chem.*, 1986, **58**, 2486–2492.
31 B. M. Beam, R. C. Shallcross, J. Jang, N. R. Armstrong and S. B. Mendes, *Appl. Spectrosc.*, 2007, **61**, 585–592.
32 S.-M. Tseng and C.-L. Chen, *Appl. Opt.*, 1992, **31**, 3438–3447.
33 J. E. A. M. van den Meerakker, P. C. Baarslag and M. Scholten, *J. Electrochem. Soc.*, 1995, **142**, 2321–2325.
34 R. Swanepoel, *J. Phys. E*, 1983, **16**, 1214–1222.
35 J. C. Manifacier, J. Gasiot and J. P. Fillard, *J. Phys. E*, 1976, **9**, 1002–1004.

36 W. J. Doherty, R. J. Wysocki, N. R. Armstrong and S. S. Saavedra, *Macromolecules*, 2006, **39**, 4418–4424.
37 W. J. Doherty III, R. J. Wysocki, N. R. Armstrong and S. S. Saavedra, *J. Phys. Chem. B*, 2006, **110**, 4900–4907.
38 K. Bergmann and C. T. O'Konski, *Nature*, 1963, **67**, 2169–2177.
39 G. Hahner, A. Marti and N. D. Spencer, *J. Phys. Chem.*, 1996, **104**, 7749–7757.
40 X. Chen and O. Inganas, *J. Phys. Chem.*, 1996, **100**, 15202–15206.
41 E. E. Bancroft, H. N. Blount and F. M. Hawkridge, *Biochem. Biophys. Res. Commun.*, 1981, **101**, 1331–1336.
42 P. E. Smolenyak, R. A. Peterson, D. R. Dunphy, S. B. Mendes, K. W. Nebesny, D. F. O'Brian, S. S. Saavedra and N. R. Armstrong, *J. Porphyrins Phthalocyanines*, 1999, **3**, 620–633.
43 B. M. Beam, Ph.D. Dissertation, University of Arizona, 2008.